Potential field modelling of the Tingha Monzogranite and tin mineralised Gilgai Granite, Inverell NSW

Astrid Carlton
Geological Survey of New South Wales
516 High St, Maitland 2320 NSW, Australia
astrid.carlton@industry.nsw.gov.au

SUMMARY

The Gilgai Granite and the Tingha Monzogranite are located south of Inverell in northeastern NSW (see Figure 1). Potential field data has been modelled to determine the morphological relationship of these two granites. Total Magnetic Intensity (TMI) data, acquired by the NSW government Discovery 2000 program, was used to generate a 2.5D model. Presented within this paper are the results of modelling the southwestern corner of the Gilgai Granite, which accounts for approximately one third of the Gilgai Granite that is visible in TMI imagery.

The Gilgai Granite is highly mineralised with disseminated and vein-type cassiterite and polymetallic sulfide occurrences. Tin has been historically mined, mainly from shallow workings. Better understanding the mineralisation and formation controls may increase exploration in this area.

Eleven TMI cross-sections were modelled. The results indicate that the Gilgai Granite is steeply dipping and tapers with increasing depth. It has a vertical extent of approximately 1000–1400 m and intruded around and over the Tingha Monzogranite, but not beneath the Tingha Monzogranite. The Gilgai Granite has sill-like bodies, isolated masses and/or roof pendants that intrude the Tingha Monzogranite. The source rock has magnetic zonation, with modelled magnetic susceptibilities ranging from $4.8–14.0\times10^{-3}$ SI with a mode of 5.5×10^{-3} SI.

Key words: Gilgai Granite, Tingha Monzogranite, aeromagnetic, tin mineralisation.

INTRODUCTION

The Tingha and Gilgai granites lie within the central block of the New England Orogen. Exploration in this area has been hampered by a lack of understanding of mineralisation controls and conceptual models (Brown, 2006). Modelling the Gilgai Granite, using aeromagnetic data, will increase our understanding of the 3D morphological relationship between the Tingha and Gilgai granites. The morphology will show intrusive relationships and provide an indication of the vertical extent of the Gilgai Granite. The bottom depths of the modelled sources will indicate whether the granite is laccolithic, eroded remnants or depth extensive. The results may have an effect on the prospectivity of the granite, i.e. there may be more Sn mineralisation if the granite is not laccolithic.

The morphology of the underside of the sources will indicate whether the Gilgai Granite is emplaced under the Tingha Monzogranite. Juniper and Kleeman (1979) comment that 'spatial relationships in mineshafts indicate that the Gilgai Granite has been emplaced under the Tingha' Monzogranite. They also suggest that the roof of the Gilgai Granite is just being exposed as chemically equivalent porphyries, which have been intruded by the Gilgai Granite, are considered to be the extrusive equivalents of the Gilgai Granite.

Figure 1. Location map for the Tingha and Gilgai granites with regional geology transparently overlaid on greyscale tilt-filtered TMI imagery. Main roads are marked in black lines. All coordinates are in GDA94 MGA zone 56.

Magnetic modelling of the Gilgai Granite is an efficient method to elucidate the morphological relationship between the Tingha and Gilgai granites as (1) high resolution aeromagnetic data is available, (2) the Gilgai Granite has complex and higher TMI signature than the Tingha Monzogranite and (3) we have numerous magnetic susceptibility readings of outcropping samples for both granites to provide constraints on the models.

The Gilgai (-Rgil) and Tingha (P-Rgtg) granites form a roughly circular, composite pluton about 70 km in diameter

(see Figure 1). They intrude Early Carboniferous metasediment (DCss, the Sandon beds) to the north and south, Early Permian Bundarra Supersuite (Pgbd) to the west and Late Permian felsic volcanic Wandsworth Volcanic Group (Pfw) to the east (Brown & Stroud 1998 and Brown et al., 1990). The geological boundaries in Figure 1 are from mapping completed before aeromagnetic data was acquired. The new imagery shows some areas that are incorrectly mapped.

The Tingha Monzogranite (previously called the Tingha Adamellite) has a SHRIMP U-Pb date of 251.3 ± 1.7 Ma (Blevin, 2010) and is relatively non-magnetic ($3–20\times10^{-5}$ SI). It is a porphyritic, hornblende-biotite monzogranite (GA Stratigraphic Unit Database) within the Uralla Supersuite and exhibits both S- and I-type characteristics (Brown & Stroud, 1993).

The Gilgai Granite has a SHRIMP U-Pb date of 252.2 ± 1.8 Ma, 252.6 ± 1.8 Ma and 251.8 ± 1.7 Ma (Blevin, 2010) and is relatively non-magnetic to magnetic ($3–438\times10^{-5}$ SI). It is fine- to coarse-grained, equigranular to porphyritic, biotite leucogranite (Stroud & Brown, 1998) that is strongly fractionated with I-type characteristics (Brown & Stroud, 1993). It has district scale zoning. Silver and base metal-rich lodes occur within 4–6 km of the western margin while tin-rich lodes occur largely near the centre of the composite pluton (Brown & Stroud, 1993). Juniper and Kleeman (1993) state 'transitional lithologies are apparent near contacts with the Tingha Adamellite probably indicating local digestion of the host rock'. Recent age dates suggest the granites formed almost synchronously, indicating that these transitional lithologies are hybrids where magmatic fluids mixed (Blevin, 2010).

Over 200 cassiterite lodes have been recognised (Brown & Stroud, 1993) in the Gilgai Granite, with minor As, Fe, Cu, W and Mo sulfides and or oxides. Mineralisation is genetically related to the Gilgai Granite, occuring along pre-existing joints and in contacts with the Gilgai Granite. Historically Sn has been mined mainly from alluvial and deep lead cassiterite, with numerous small lode Sn deposits. Current Sn prices dictate exploration for further Sn deposits.

It is the author's intention that the whole of the Gilgai Granite is modelled (where there is a TMI signal). The preliminary results presented here represent approximately a third of the area that can be modelled. The results indicate that the Gilgai Granite intruded around and over the Tingha Monzogranite, but no Gilgai Granite is emplaced beneath the Tingha Monzogranite.

METHOD AND RESULTS

Magnetic modelling was completed using an aeromagnetic TMI grid generated from data flown for CRA Pty. Limited (Gwydir survey). This grid was used to generate cross-section lines for modelling. The flight line data could not be used directly in the modelling as they do not traverse the circularly-shaped Gilgai Granite perpendicular to the strike its anomaly (for the most part). The survey was flown on east–west flight lines with a 250 m line spacing. The survey specifications stated a nominal 60 m ground clearance. Examination of the radar altimeter channel showed ground clearance from approximately 60 to 120 m. The height of the magnetometer

sensor is a critical component in modelling the depth of a source. To compensate for the varying depth a grid was generated in Geosoft® Oasis Montaj using the radar altimeter channel in the flight line data. This was then imported into Encom™ ModelVision™ 10.0, along with the TMI grid. Radial traverses where then used to generate cross-section lines for magnetic modelling (lines A–I as shown in Figure 2). The modelling was conducted with polygons and tabular bodies, using a combination of manual operation and an inversion tool.
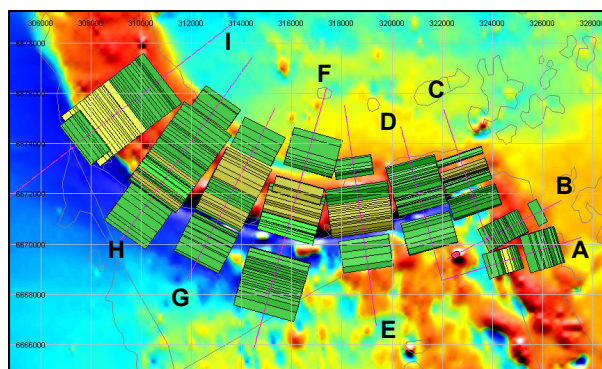

Figure 2. Location of modelled cross-sections A–I and the source bodies generated. Bodies are colour-coded by magnetic susceptibility, see Table 1. Background image is pseudocolour TMI with regional geological boundaries outlined in grey.

The initial magnetic susceptibilities entered were based on the measured samples from outcrop. All of these samples have been weathered to varying degrees. The inversion results, listed in Table 1, indicate that the magnetic susceptibility (k) of deeper, unweathered source rocks is higher than those that outcrop. The mode susceptibility is 5.5×10^{-3} SI. This is primarily attributed to magnetite and a small amount of pyrrhotite.

Body	k	Body	k	Body	k	Body	k
A1	5.5	D2	5.2	F5	6.5	H2	5.5
A2	8.0	D3	4.8	F6	6.5	H3	6.9
A3	4.8	E1	5.5	F7	5.5	H4	12.0
B1	5.5	E2	6.1	G1	5.5	H5	6.5
B2	5.5	E3	4.8	G2	5.5	H6	14.0
C1	5.5	E4	4.8	G3	7.4	H7	5.0
C2	5.5	F1	5.0	G4	12.0	H8	5.0
C3	6.9	F2	5.5	G5	6.0	I1	5.5
C4	5.5	F3	11.0	G6	5.0	I2	9.5
D1	5.5	F4	5.5	H1	5.0	I3	5.0

Table 1. Modelled magnetic susceptibility ($k\times10^{-3}$) for each source body, k-values are colour coded, 4.0–5.9 are forest green, 6.0–7.9 are khaki, 8.0–9.9 are spring green and 10.0> are lime green.

Modelled cross-sections A and B (figures 2 & 4) are over part of the Gilgai Granite that is incorrectly mapped in Figure 1 as Tingha Monzogranite. The models indicate sill-like bodies to the east of the main Gilgai Granite body.

Modelled cross-sections C to I (figures 5–11) are situated over the southwestern portion of the Gilgai Granite and indicate a steeply dipping contact with the Bundarra Supersuite (bodies C1, D2, E2, F3, F4, G2, H2 and I2). The dip of the contact is towards the Tingha Monzogranite.

The dip of the contact with the Tingha Monzogranite (bodies C3, D3, E3, F4, F6 and H7) is generally gentler, except in cross section I (body I3, see Figure 11), where it is near vertical. These contacts dip towards the Gilgai Granite, except cross-section G (Figure 9) where body G3 dips towards the Tingha Monzogranite. In cross-sections C, D, E and H the modelled source bodies C3, D3, E3, F6 and H7 intrude over the Tingha Monzogranite. These are interpreted as parts of Gilgai Granite roof, which indicates that the Gilgai Granite intruded around and over the Tingha Monzogranite. Modelled cross-sections without a source body intruding over the Tingha Monzogranite are interpreted as areas where the roof has been eroded (A, B, G and I, see Figures 3, 4, 9 and 11).

Bodies C1, D1, E1, F1, F2, G1 and H1 are located to the southwest of the mapped boundaries of the Gilgai Granite; they are likely to be metamorphic aureoles.

Modelled cross-sections E, F, G and H have sill-like bodies (E4, F7, G6 and H8) on the Tingha Monzogranite side of the cross-section. Alternatively it is possible that these bodies represent roof pendants. Body C4 is interpreted as a roof pendant or an isolated mass as its morphology is not sill-like.
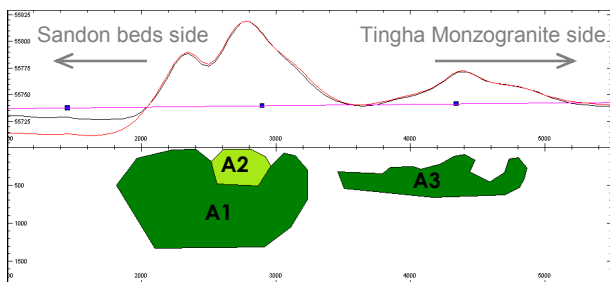
Figure 3. Modelled TMI cross-section of Line A. The red line represents the modelled TMI field, the black line is the observed aeromagnetic TMI data and the fuchsia is the calculated regional TMI field. The top half of the Y-axis is the TMI field (nT) whilst the lower half is the depth below the surface (m). The x-axis is the distance along the cross-section (m).

Thrust faulting within the Gilgai Granites has been interpreted in cross-sections B and F (Figures 4 & 8) from the morphology of the modelled source bodies.
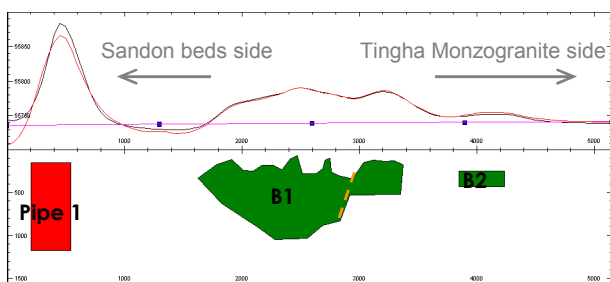
Figure 4. Modelled TMI cross-section of Line B. Line colours and axes represent the same units as in Figure 3. The dashed orange line represents an interpreted thrust fault.
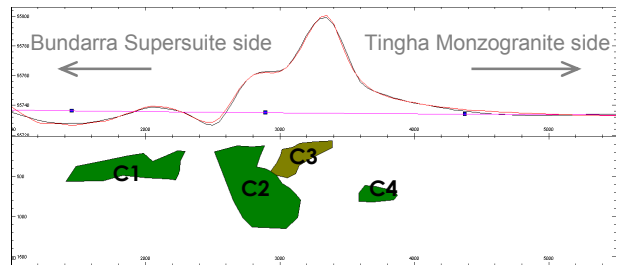

Figure 5. Modelled TMI cross-section of Line C. Line colours and axes represent the same units as in Figure 3.

Between source D2 and D3 is a region of low or non-magnetically susceptible material. This region is interpreted as representing the non-magnetic samples of Gilgai Granite collected. This region is visible, on a smaller scale, in all the other cross-sections. It is evident as a gap between modelled sources or undulating morphology on the top side of a source body (i.e. B1, I2, I3).
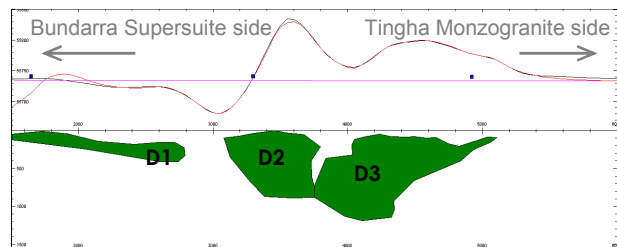

Figure 6. Modelled TMI cross-section of Line D. Line colours and axes represent the same units as in Figure 3.
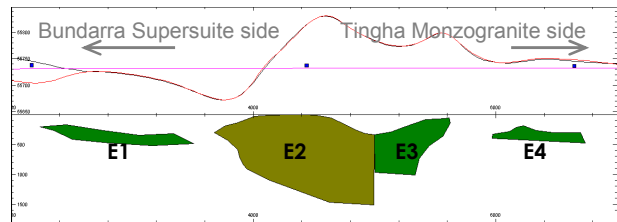

Figure 7. Modelled TMI cross-section of Line E. Line colours and axes represent the same units as in Figure 3.
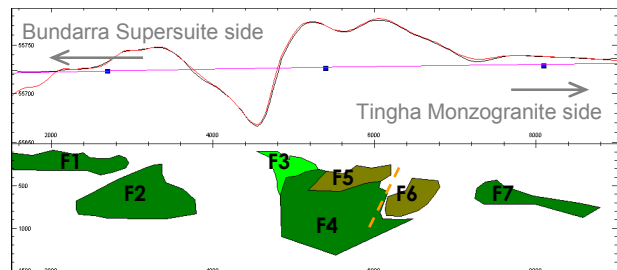

Figure 8. Modelled TMI cross-section of Line F. Line colours and axes represent the same units as in Figure 3.

The vertical depth extent for the Gilgai Granite is approximately 1000–1400 m (excluding the adjacent interpreted sill-like, roof pendant-like and aureole sources). Most of the sources that comprise the Gilgai Granite (A1, B1, C2+C3, CD+D3, E2+E3, F+F4+F5+F6, H2+H3+H4+H5+H6+H7 and I1+I2+I3) taper with increasing depth. The morphology of the modelled sources does not indicate that the Gilgai Granite extends under the Tingha Monzogranite. Juniper and Kleeman (1979) do not state

depths or locations for the spatial relationships in the mineshafts that indicated to them that the Gilgai Granite has been emplaced under the Tingha Monzogranite. It is possible that they did not explore as deeply as in this modelling.
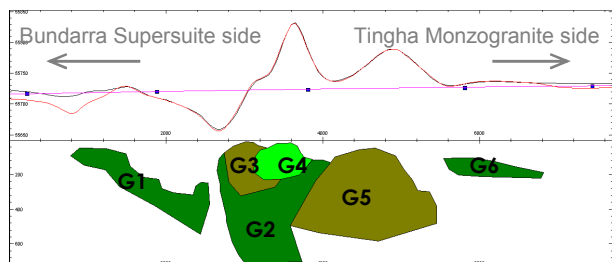

Figure 9. Modelled TMI cross-section of Line G. Line colours and axes represent the same units as in Figure 3.
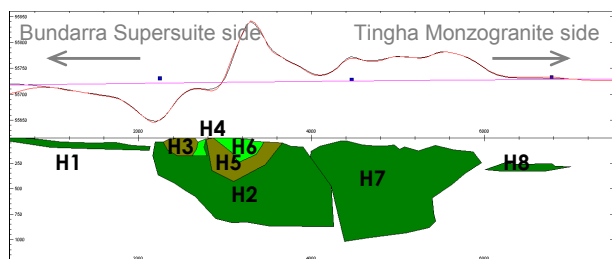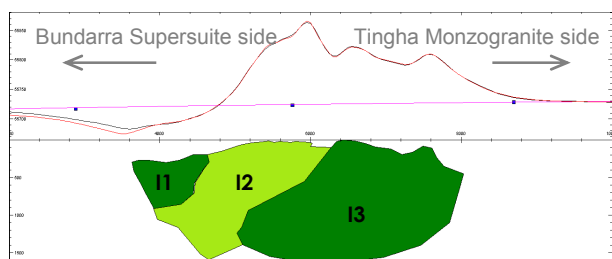

Figure 10. Modelled TMI cross-section of Line H. Line colours and axes represent the same units as in Figure 3.

Figure 11. Modelled TMI cross-section of Line I. Line colours and axes represent the same units as in Figure 3.

CONCLUSIONS

The Gilgai Granite is interpreted to have intruded around and over the Tingha Monzogranite. It has interpreted sill-like bodies and isolated masses (or preserved roof pendants) that intruded the Tingha Monzogranite. The Gilgai Granite tapers with increasing depth and does not extend under the Tingha Monzogranite, as previously suggested by Juniper and Kleeman (1979).

The Gilgai Granite is not laccolithic, with a maximum vertical extent of approximately 1000–1400 m. Mineralised economic minerals similar to those exposed at the surface, may exist within the body.

The modelling indicates a complex geometry, with steeply dipping contacts, thrust faults, zonation of magnetic susceptibilities and higher magnetic susceptibilities than those measured from surface samples. Further modelling is expected to support these findings.

REFERENCES

Blevin, P.L., 2010, Old friends in a whole new light: A new chronology for the igneous metallogeny of the southern New England Orogen, New South Wales. *In*: Buckman, S. and Blevin, P.L., *eds*., New England Orogen 2010 conference proceedings, 45–48.

Brown, R.E., 2006, Inverell *Exploration NSW* geophysics — new data for exploration and geological investigation in the northern New England area of New South Wales: *Geological Survey of NSW, Quarterly Notes* 121.

Brown, R.E., Krynen, J.P. and Barlow, J.W., 1990, Manilla – Narrabri 1:250 000 Metallogenic map. Geological Survey of New South Wales, Sydney.

Brown, R.E and Stroud, W.J., 1993, Mineralisation related to the Gilgai Granite, Tingha–Inverell area. *In*: Flood, P.G. and Atichison, J.C., *eds*., New England Orogen, eastern Australia, NEO '93 conference proceedings, University of New England, 431–447.

Geoscience Australia Stratigraphic Units Database, accessed 2011, http://dbforms.ga.gov.au/www/geodx.strat_units.int

Juniper, D.N. and Kleeman, J.D., 1979, Geochemical characterisation of some tin-mineralizing granites of New South Wales. Journal of Geochemical Exploration, Vol 11, 321–333.

Stroud, W.J. and Brown, R.E., 1998, Inverell 1:250 000 Metallogenic Sheet SH/56-5. First Edition. Geological Survey of New South Wales, Sydney.